AAPS PharmSciTech (2024) 25:39
https://doi.org/10.1208/s12249-024-02740-x

RESEARCH ARTICLE

Novel Approaches for Cutaneous Pharmacokinetics

Predicting Human Dermal Drug Concentrations Using PBPK Modeling and Simulation: Clobetasol Propionate Case Study

William W. van Osdol[1] · Jasmina Novakovic[1] · Maxime Le Merdy[1] · Eleftheria Tsakalozou[2] · Priyanka Ghosh[2] · Jessica Spires[1] · Viera Lukacova[1]

Received: 25 October 2023 / Accepted: 8 January 2024 / Published online: 17 February 2024

Abstract

Quantitative *in silico* tools may be leveraged to mechanistically predict the dermato-pharmacokinetics of compounds delivered from topical and transdermal formulations by integrating systems of rate equations that describe permeation through the formulation and layers of skin and pilo-sebaceous unit, and exchange with systemic circulation via local blood flow. Delivery of clobetasol-17 propionate (CP) from Dermovate™ cream was simulated using the Transdermal Compartmental Absorption & Transit (TCAT™) Model in GastroPlus®. The cream was treated as an oil-in-water emulsion, with model input parameters estimated from publicly available information and quantitative structure-permeation relationships. From the ranges of values available for model input parameters, a set of parameters was selected by comparing model outputs to CP dermis concentration-time profiles measured by dermal open-flow microperfusion (Bodenlenz *et al*. Pharm Res. 33(9):2229–38, 2016). Predictions of unbound dermis CP concentrations were reasonably accurate with respect to time and skin depth. Parameter sensitivity analyses revealed considerable dependence of dermis CP concentration profiles on drug solubility in the emulsion, relatively less dependence on dispersed phase volume fraction and CP effective diffusivity in the continuous phase of the emulsion, and negligible dependence on dispersed phase droplet size. Effects of evaporative water loss from the cream and corticosteroid-induced vasoconstriction were also assessed. This work illustrates the applicability of computational modeling to predict sensitivity of dermato-pharmacokinetics to changes in thermodynamic and transport properties of a compound in a topical formulation, particularly in relation to rate-limiting steps in skin permeation. Where these properties can be related to formulation composition and processing, such a computational approach may support the design of topically applied formulations.

Keywords critical quality attributes · dermal pharmacokinetics · modeling and simulation · PBPK · topical formulation design

Introduction

Dermatological drug products are used to treat skin diseases such as psoriasis, acne, atopic dermatitis, and infections [1]. Development and assessment of local bioavailability of such products face significant challenges as the active pharmaceutical ingredients (APIs) from these drug products reach the site of action (skin layers) before they enter systemic circulation. Furthermore, these topical administrations usually produce very low to undetectable systemic exposure.

Consequently, within the scope of bioequivalence (BE) assessment standard pharmacokinetic approaches based on comparing systemic drug concentrations between the reference standard (RS) and its generic are typically not

Communicated by M. Alice Maciel Tabosa, Jaimin R. Shah, Sharareh Senemar, and Nisarg Modi

✉ Jessica Spires
jessica.spires@simulations-plus.com

[1] Simulations Plus, Incorporated, 42505 10th Street West, Lancaster, California 93534, USA

[2] Office of Research and Standards (ORS), Office of Generic Drugs (OGD), Center for Drug Evaluation and Research (CDER), U.S. Food and Drug Administration (FDA), Silver Spring, Maryland, USA

applicable, and comparative clinical endpoint studies or *in vitro* characterization based BE approaches may be considered instead [2–5]. The advantage of comparative clinical endpoint trials is their ability to assess the efficacy of the drug product. However, those trials may require large numbers of subjects, are time-consuming, costly, and often less sensitive to formulation differences between a prospective generic drug product and the corresponding RS [6]. Hence, there are challenges limiting the development of generic drug products. To address challenges with the development of generic drug products applied to the skin, the U.S. Food and Drug Administration (FDA) is funding research on methodologies that are able to assess the *in vitro* and *in vivo* performance of topical drug products applied to the skin. These include, but are not limited to, *in vitro* permeation testing, *in vivo* dermal microdialysis, dermal open flow microperfusion (dOFM), and *in silico* models [7].

Quantitative methods and modeling, such as physiologically based pharmacokinetic (PBPK) models, have been identified to support alternative BE approaches [2, 8]. Indeed, dermal PBPK models provide an insight into drug partitioning within the skin layers by linking the API and formulation physicochemical and structural (Q3) properties with skin physiology. Recently, dermal PBPK modeling supported the approval of a generic diclofenac topical gel. The approval was based on the totality of evidence: qualitative (Q1) and quantitative (Q2) sameness as well as the Q3 similarity of the generic to the RS, an *in vivo* PK BE study, and PBPK-based virtual BE analysis [2, 9]. Although this generic approval represents a breakthrough in regulatory decision making for locally acting generic drug products, more research is needed to improve the predictability of PBPK models. To that effect, enhancement of PBPK models for complex routes of delivery remains a priority of the Generic Drug User Fee Amendments (GDUFA) Program [10].

A skin absorption model was developed and validated to simulate the permeation of small molecules based on their physicochemical properties and formulations characteristics. The aims of the work presented here were to use this dermal PBPK model to [11] predict clinically observed concentration-time profiles of clobetasol-17 propionate (CP) formulated in Dermovate™ cream, 0.05% obtained using the dOFM technique. (1); and [1] correlate local dermis exposure with Dermovate™ cream, 0.05% (GlaxoSmithKline Pharma, GmBH, Vienna, Austria) formulation properties. This product was identified as a case study based on the availability of clinical dermal CP concentration-time profiles using the dOFM technique to examine skin permeation. The Dermovate formulation of CP is also well characterized in the literature. As such, the drug product characteristics were informed experimentally in the developed model and model predictions of local bioavailability were assessed against observed data rendering this an ideal case study for modeling skin absorption using *in silico* methods.

This article describes (i) development and calibration of the dermal PBPK model for CP; (ii) application of this model to predict CP concentration-time profiles in layers of the dermis; and (iii) parameter sensitivity analyses (PSA) to illustrate the impact of formulation differences between hypothetical formulation variants on local and systemic CP exposure.

Methods

Skin Absorption Model

The Transdermal Compartmental Absorption and Transit (TCAT™) Model within the software application GastroPlus® (version 9.8.2, Simulations Plus Inc., Lancaster, CA, USA) was used for numerical simulation of CP biodistribution in human skin layers. The model describing skin drug absorption and disposition was linked with a one-compartment pharmacokinetic model to capture systemic distribution and clearance of CP.

Model Structure

The structure of the skin absorption model is shown schematically in Figure S1 of the Supplementary Information. The model comprises a set of compartments, connected in series and parallel by diffusive mass exchange, to represent the stratum corneum (SC), viable epidermis (VE), dermis, subcutaneous tissue (SQ), sebum, hair lipid, and hair core. Topical and transdermal dosage forms applied to the SC surface are represented by the vehicle compartment.

The model treats diffusion in time and a single spatial dimension by imposing a mass transfer boundary condition between compartments that approximates diffusive flux due to concentration gradients. To treat concentration gradients that may develop within them, the formulation and skin compartments, with the exception of the subcutaneous tissue, can be divided into sub-layers. Each skin and pilosebaceous sub-layer is assumed to be homogeneous, and each thermodynamic phase of a formulation sub-layer is assumed to be homogeneous. The number of sebum sub-layers equals the number of VE plus dermis sub-layers, and the number of internal hair sub-layers equals the sum of SC, VE and dermis sub-layers. Equations for the exchange of mass among model compartments and between successive sub-layers of a given model compartment are presented in the Supplementary Information, Equations (4)–(11).

After application to the skin, the drug and excipients comprising a formulation undergo a variety of processes that result in absorption, distribution, and clearance. At present, the model encompasses the following processes:

- Evaporation of a volatile drug and excipient
- Equilibrium binding of the permeant in each skin and pilosebaceous compartment (as % bound)
- Linear and nonlinear binding to melanin in the VE and hair core
- Linear (non-saturable) clearance (degradation) in the VE, dermis, and SQ
- Exchange with the systemic circulation via blood flow to the dermis and SQ, and lymph flow in SQ (relevant principally for compounds with molecular weight greater than about 20 kilodaltons)

Details about the equations defining these processes are provided in the Supplementary Information.

Clobetasol-17 Propionate (CP)

CP, a halogenated derivative of prednisolone, is a highly potent topical corticosteroid. First approved by the FDA in 1985 as cream and ointment formulations [12], it is used to relieve inflammatory and pruritic manifestations of steroid responsive dermatoses, such as psoriasis and other skin conditions, which do not respond satisfactorily to less potent corticosteroids [13]. Continuous use of CP is dose- and duration-limited ($\leq$ 50 g/week for $\leq$ 4 weeks) to avoid suppression of the hypothalamic-pituitary-adrenal axis [12]. In addition to the cream and ointment, CP is currently available as a gel, lotion, solution, spray, shampoo, and aerosol foam. CP has a molecular weight of 467 daltons, no ionizable moieties, a logP ~ 3.5 [14] and water solubility ~ 3.6 mg/mL [15].

Model Input Parameters

We developed a dermal PBPK model for Dermovate cream, 0.05% ("Dermovate cream") and used the Day 1 dermis CP concentration-time profiles and *AUC*s from non-lesional skin of psoriasis patients in the dOFM clinical study reported by Bodenlenz *et al.* [11] to assess model performance. Simulated dose and application area per site were set to those of the clinical study: 15 mg cream/cm^2 skin, and 7.7 cm^2 skin, respectively.

Values for the biopharmaceutic and physicochemical parameters that characterize the cream were obtained primarily from the work of Kasongo and Fauzee [15, 16]. The composition of the cream is provided in Table I. Volume fractions of CP and formulation excipients were estimated from density information available at PubChem and manufacturer websites. The density of Dermovate cream was estimated to be 1 g/mL.

For modeling purposes, we treated the cream as a two-phase oil-in-water emulsion. Fauzee discussed the possibility that lamellar lipid phases also exist within the formulation [16, 17], but the actual phase structure of Dermovate cream has not been determined experimentally. Values of model input parameters, their units, and sources or methods of derivation are summarized in Table II.

CP release from the Dermovate cream, measured under occlusion and through 0.1 mm polycarbonate or 0.025 mm nitrocellulose membranes [15, 16], were used to estimate the apparent diffusivity of CP (D_{eff}) in the continuous phase of the cream. Analyzing the release data via Higuchi's equation and an approximate equation for release at short times, we obtained D_{eff} ~ 2.6e-8 and 4.5e-9 cm^2/s, respectively [18]. CP release from propylene glycol: water 50:50 v/v solutions was much more rapid than from the cream, but release rates from the cream did depend on membrane composition and pore size suggesting that the synthetic membranes used in the study influenced the observed CP release rate

Table I Weight Percent Composition of Dermovate Cream [16]

Component	% (w/w)	% (v/v)	PubChem CID	Phase
Propylene glycol	47.5	45.4	1030	Continuous aqueous
Distilled water	30.2	30.2	962	
Sodium citrate	0.05	2.99E-02	6244	
Citric acid	0.05	2.99E-02	311	
Glyceryl monostearate	11.0	11.3	24699	Dispersed hydrophobic
White beeswax	1.15	1.18	*	
Cetostearyl alcohol	8.40	10.3	62238	
Arlacel 165	1.50	1.54	**	
Chlorocresol	0.075	5.44E-02	1732	
Clobetasol-17 propionate	0.05	4.10E-02	32798	Partitions

*https://www.sigmaaldrich.com/

**https://www.crodapersonalcare.com/

Table II Model and Systemic PK Input Parameter Values and Their Sources or Derivations. Alternate Values Available for some Input Parameters were Explored through Parameter Sensitivity Analysis, as Described in the Text

Parameter	Value	Units	Sources, definitions, derivations
Cream composition			AYB Fauzee, MS Thesis [16]
CP content	0.5	mg/g cream	Dermovate cream prescribing information [13]
Dispersed phase volume fraction, j_{disp}	0.244		Calculated from the composition and density information
CP solubility in water	4.06E-03	mg/mL	KW Kasongo MS Thesis [15]
Continuous phase solubility	0.397	mg/mL	KW Kasongo MS Thesis [15]
Cont phase/water partition coeff, $K_{cont,w}$	97.9		Calculated as the ratio of the respective solubilities
Disp phase/water partition coeff, $K_{disp,w}$	357		Baseline value: $K_{veg\ oil,w} = 1.115*LogP - 1.35$ [27]
Disp phase/water partition coeff, $K_{disp,w}$	3162		Alternate value $K_{o,w} = 10^{LogP}$
CP Diffusivity in water, D_w	5.90E-06	cm^2/s	ADMET Predictor 10.3
Cont phase effective diffusivity, D_{eff}	2.61E-08	cm^2/s	*In vitro* release data using Higuchi's equation (15,16,18)
Dispersed phase diffusivity, D_{disp}	4.25E-09	cm^2/s	Cyclic voltammetry & scaling by CP hydrodynamic radius [22]
Dispersed phase droplet radius, r_{disp}	1	µm	A representative value for emulsion-based creams
Diffusion length scale, h_{mem}	0.01	µm	Figures in dispersed ↔ continuous phase diffusive mass transfer
Adhesion thickness	1E-04	µm	Determines skin surface area covered by dispersed phase
SC thickness	13	µm	Model default value for human arm skin
VE thickness	61.4	µm	
Dermis thickness	1131	µm	
Subcutaneous tissue thickness	2642	µm	
CP SC diffusivity, D_{SC}	1.10E-11	cm^2/s	Wilschut, A *et al.* [24]
SC/water partition coeff, $K_{SC,w}$	22.52		
SC permeability, P_{SC}	1.91E-07	cm/s	
VE diffusivity, D_{VE}	1.26E-06	cm^2/s	Kretsos, K, *et al.* [25]
VE/water partition coeff, $K_{VE,w}$	0.70		
VE permeability, P_{VE}	1.44E-04	cm/s	
Dermis diffusivity, D_{de}	1.26E-06	cm^2/s	Kretsos, K, *et al.* [25]
Dermis/water partition coeff, $K_{de,w}$	0.70		
Dermis permeability, P_{Dermis}	7.82E-06	cm/s	
Sebum diffusivity, D_{Sebum}	3.28E-09	cm^2/s	Yang S, Lian G, *et al.* [28]
Sebum/water partition coeff, $K_{Sebum,w}$	556		Yang S, Lian G, *et al.* [29]
Sebum permeability, P_{Sebum}	1.53E-05	cm/s	Model/Gastro Plus 9.8.3
CP bound in VE & Dermis	84	%	Kretsos, K, *et al.* [25]
Blood flow in the dermis, Q_{dermis}	9.89E-02	mL/min/g skin	Model default for human arm skin
Blood flow in subcutaneous tissue, Q_{SQ}	2.60E-02	mL/min/g SQ	Model default for human arm skin
Systemic clearance, CL_{sys}	4	L/h	ADMET Predictor 10.3
Volume of distribution, $V_{d,c}$	2.54	L/kg	ADMET Predictor 10.3
Plasma half-life, $t_{1/2}$	31	hours	ADMET Predictor 10.3
Blood-to-plasma concentration ratio, R_{bp}	0.77		ADMET Predictor 10.3
Fraction unbound in plasma, $F_{u,p}$	3.46	%	ADMET Predictor 10.3

[15]. Linearity of release with the square root of time was observed, but we believe these should be considered low estimates of D_{eff}.

A theoretical estimate, D_{eff} ~ 7.56e-7 cm^2/s, was obtained by starting with CP diffusivity in water, D_w ~ 5.9e-6 cm^2/s (ADMET™ Predictor 10.3, Simulations Plus, Lancaster, CA, USA), then applying the Stokes-Einstein equation to account for the viscosity of the water-propylene glycol (PG) vehicle [19], and lastly treating dispersed phase droplets as semi-permeable obstacles to CP diffusion [20, 21].

The model treats mass transfer between the continuous and dispersed phases of Dermovate cream in similar fashion to diffusion between any other distinct compartments (Equations (4)–(7) in the Supplementary Information). CP diffusivity in the hydrophobic dispersed phase (D_{disp}) was estimated from values for the diffusivity of ferrocene derived

from cyclic voltammetry measurements in microemulsions of similar hydrophobic phase composition [22]. Ferrocene, with logP ~ 2.66 [23], partitions preferentially into the dispersed phase so that the derived diffusion coefficients are thought to be representative of that phase. To obtain a value of D_{disp} for CP in Dermovate cream, we scaled the ferrocene value by the ratio of hydrodynamic radii for the two molecules.

The model treats dispersed phase droplets as homogeneous compartments, ignoring gradients that might develop within them. However, a value of the diffusion length scale, h_{mem}, in Equation (4) is needed. A default value of 0.01 mm is provided (discussed in the Supplementary Information), which users can change. Exploring a range of values from 0.01 to 0.5 mm in simulations of both CP skin permeation *in vivo* and rapid CP release *in vitro*, we found that the model predicted equilibrium partitioning of CP between dispersed and continuous phases of the emulsion. Thus, we retained the default value for the simulations presented here.

The model also treats diffusive exchange directly between dispersed phase droplets and the SC, sebum and hair lipid to which the droplets may adhere. The extent of skin and appendageal coverage by the dispersed phase is determined by the proximity required for droplets to adhere (the adsorption thickness, with a default value of 1Å) and the degree to which adhering droplets wet the respective surfaces. Using the default value of adsorption thickness, the model predicts a vanishingly small fraction of skin coverage by the dispersed phase of Dermovate cream (~ 2e-5), and thus a negligible contribution to skin permeation. In the current version of the TCAT Model and based on the operating assumptions discussed above with respect to h_{mem}, the rate of skin permeation predicted by the model is independent of the fraction of surface area covered by the dispersed phase, due to the rapid equilibration of CP between the continuous and dispersed phases.

The SC and dermis were divided into 20 sub-layers, and the formulation and viable epidermis into 10 sub-layers, to account for concentration gradients that might develop within them, and for diagnostic purposes. In certain cases, diffusive transport may be substantially more rapid in the formulation and VE than in the SC, leading to significant concentration gradients only in the latter. Gradients may also develop in the dermis because of its thickness.

The Robinson [24] and Kretsos [25] equations available in the model were used to estimate CP permeability in the SC, VE, and dermis (1.91e-7, 1.44e-4 and 7.83e-6 cm/s, respectively). The predicted value of SC permeability is within 2-fold of that reported by Siddiqui *et al.* [26] for betamethasone-17 valerate (3.64e-7 cm/s), a steroid similar to CP in structure, molecular weight, and logP.

The extent of CP binding to protein and lipid in the dermis ($f_{b,dermis}$) was estimated to be 84% using the model developed by Kretsos *et al.* [25]; in particular experimental data for progesterone and testosterone binding to human serum albumin in aqueous solution presented in Table 2 of that publication, and intermediate model calculations for several steroids presented in Table 4 of that publication.

The following processes were not incorporated into the model for Dermovate cream due to limitations in the model itself or due to lack of sufficient information with which to implement quantitative treatment:

- Water and PG permeation through the SC, and their potential to enhance CP permeation
- Evaporation of water from Dermovate cream and its effects on CP skin permeation due to dynamic changes in solubility as water evaporates from the formulation
- Vasoconstriction caused by CP that reduces blood flow to the dermis, Q_{dermis}

Tracking of multiple permeating and interacting species that can modulate API permeation through the SC should be prioritized in future computational modeling of skin permeation.

Systemic PK Model

To the best of our knowledge, the intravenous pharmacokinetics of CP have not been determined experimentally in man. Following dermal application in patients with psoriasis or atopic dermatitis, the compound is absorbed systemically, with plasma levels reaching high pg/mL to low ng/mL levels (depending on dosing details) and with great inter-individual variability [30, 31].

A one-compartment pharmacokinetic model for systemic CP distribution and elimination was used. Parameter values were estimated from the canonical SMILES string (PubChem) by ADMET Predictor 10.3. These values are also listed in Table II.

Dermal Open Flow Microperfusion

In the clinical case study of Dermovate cream reported by Bodenlenz *et al.*, the formulation was applied once daily for 14 days to small lesional and non-lesional sites on the arms of eight psoriatic patients. On Days 1 and 14, dermis concentration profiles were measured continuously in triplicate for 24 h by dOFM [11]. On Days 2–13, the duration of cream application was reduced from 24 to 4 h.

A pre-dose sample and six pooled post-dose samples (0–4 h, 4–8 h, …, 20–24 h) of dermis interstitial fluid were collected from the non-lesional and lesional sites of each subject and quantitated by LC-MS-MS. The CP concentrations thus determined were assigned to the mid-times of the sampling periods (2 h, 6 h, …, 22 h). The lower limit of quantitation for the method was 0.35 ng/mL.

Depths of the dOFM probes in the skin, defined as the distance from the skin surface to the upper surface of the exchange region of a probe, were measured by ultrasound. Reported values were the average of two measurements made from different points along the central exchange section of the probe [32]. To simulate average dermis concentration profiles, we approximated the depth of an individual dOFM probe by determining the sub-layer covering the reported probe depth. The sub-layer indices for each probe (24 probes in 8 subjects) were then averaged to define the sub-layers corresponding to the average probe depth and covering its 95% confidence interval.

The mean reported probe skin depth was 870 ± 90 mm, corresponding to dermis sub-layer 14 in the model, with a 95% confidence interval. When comparing simulation results to the clinical observations, mean probe center line depth, 1030 mm, might be considered more appropriate for determining the relevant dermis sub-layer (sub-layer 17 in the model). This depth is defined as mean reported probe depth plus the outer radius of the dOFM probe, 160 mm [32]. As discussed below, our simulations suggest that comparison of simulation output from the model to the clinical observations indicates that either option is acceptable.

In principle, there is no size limitation on molecular species that can be sampled by dOFM. However, if diffusion is the primary mode of exchange by which perfusate samples interstitial fluid, then unbound CP (diffusivity in water, D_w, ~ 5.9e-6 cm^2/s, Table II) should equilibrate much more rapidly than CP bound to human serum albumin (HSA) for example, since the protein's diffusivity in water is 10-fold lower [33], with the disparity perhaps even greater in the dermis extracellular matrix due to molecular sieving [34]. Thus, it is unclear to what extent CP bound to HSA should be considered in comparing simulated dermis concentration profiles to those observed clinically. For clarity and simplicity, we report simulated concentration-time profiles for unbound CP.

Per Bodenlenz *et al.*, the application sites on the arms of psoriasis patients participating in the study were protected by a non-occlusive dressing. It is not clear to the authors to what extent this dressing would impact the actual drying rate of the product post application. Additionally, experimental data characterizing the evaporation rate of the Dermovate cream is not available in the public domain. Therefore, no formulation drying was assumed in the developed PBPK model described here.

Parameter Sensitivity Analysis (PSA)

We investigated the sensitivity of model predictions to formulation parameters for which a range of plausible values existed or which might be explored during formulation development. The previously validated model was utilized for PSA while model parameters of interest were varied systematically. In particular, the sensitivity analysis focused on:

- The solubility of CP in the dispersed phase of the oil-in-water (O/W) emulsion as determined by the dispersed phase-water partition coefficient, $K_{disp,w}$
- The volume fraction of the dispersed phase, φ_{disp}
- The coupled parameters $K_{disp,w}$ and φ_{disp} (all pairs of values used in the previous analyses)
- The effective diffusivity of CP in the continuous phase of the emulsion, D_{eff}
- Mean radius of dispersed phase droplets, r_{disp}
- Dermis blood flow, Q_{dermis}

Evaporation of water from Dermovate cream and its effects on CP skin permeation due to dynamic changes in solubility as water evaporates from the formulation were not taken into consideration in these calculations but were treated in a separate analysis.

Results

Computational Model Simulation Results

Simulation results using the tabulated parameter values are shown in Fig. 1, along with average dermis concentrations of CP measured by dOFM in non-lesional skin on Day 1 of the study (N=8, with 3 probes each). Simulated unbound CP concentrations in dermis sub-layer 14 (corresponding to mean reported probe skin depth) and sub-layer 17 (corresponding to mean probe center line depth) were within two- to threefold of the mean dermal CP concentrations observed over 4 to 24 h post dose. Simulation results for sub-layers 15 and 19 (encompass the 95% confidence intervals for the measured probe center line depth (± 90 µm)) are also shown. The simulation also reproduced the qualitative features of the average observed profile rather closely.

The model predicts a long quasi-steady state over 7 to 10 days, with gradual decline thereafter. Quasi-steady total CP plasma concentrations reached ~ 5 pg/mL, with unbound concentration ~ 0.2 pg/mL (results not shown). This was well below the quasi-steady unbound CP concentration in the lowest dermis sub-layer, ~ 90 pg/mL. Thus, relative to the dermis, the rest of the body approximated an infinite sink for CP.

Bodenlenz *et al.* [11] also reported values of dermis CP $AUC_{0\text{-}24h}$ on Day 1 for individual subjects. These are plotted in Fig. 2 *versus* probe skin depth and in comparison, with predicted values of $AUC_{0\text{-}24h}$ calculated from the simulated unbound CP profiles in each dermis sub-layer. The simulated

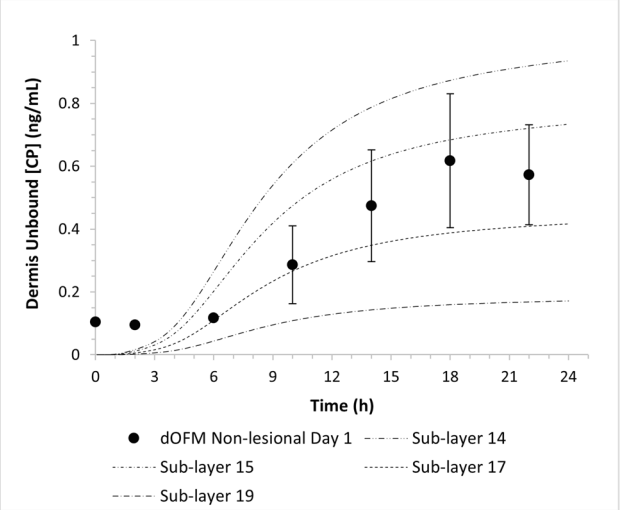

Fig. 1 Simulated concentrations of unbound CP in dermis sub-layers 14 (mean reported probe depth), 15, 17 (mean depth of probe center lines) and 19 are plotted, along with the mean interstitial fluid CP concentrations measured by dOFM in non-lesional skin sites on the arms of psoriatic patients (± SEM) (1)

AUC values passed through the range of observed values at skin depths ≳ 800 mm but appeared to exceed the distribution of measured values at shallower skin depths (500–800 mm). Bodelenz *et al.* reported a statistically significant gradient in 24-h exposure with probe depth, but one much shallower than that predicted by the computational model. This

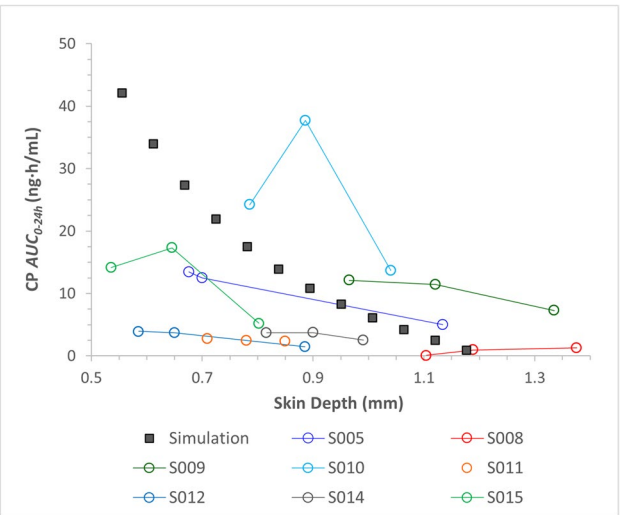

Fig. 2 Simulated (■, dermis sub-layers) and observed (open circles) unbound CP exposure in the dermis from 0 to 24 h in non-lesional arm skin, plotted *versus* skin depth. Clinical data are from non-lesional skin sites of study subjects S005, S008–S012, and S014–S015 (*N*=8, 3 dOFM probes each) on Day 1 at the reported skin depths (1). Lines connecting the data points are intended only to guide the eye

may reflect differences in the capacity for solute exchange between dermal interstitial fluid and blood, which in the model is uniformly distributed throughout the dermis, but physiologically is highest in the dermal papillae and declines with increasing depth in the dermis [35–37].

The pilosebaceous units of the model's human arm skin physiology cover only 0.144% of skin surface area in this anatomical region. Hence, one might expect the predicted contribution of the pilosebaceous pathway to CP concentrations in the viable epidermis and dermis to be small. However, as shown in Table II, sebum permeability was estimated to be 80-fold greater than SC permeability. Thus, it is not surprising that the model predicted a sebum pathway contribution of about 20% to simulated $AUC_{0\text{-}24h}$, with hair lipid and core making negligible contributions. Eliminating the sebum pathway by setting P_{sebum} to zero introduced a persistent reduction in unbound CP concentrations in dermis sub-layer 14 ($[CP]_{u,14}$) relative to the prediction including sebum permeation. In opposite fashion, increasing P_{sebum} from its estimated value raised $[CP]_{u,14}$ (results not shown). In the absence of experimental data, the validity of these predictions remains unknown.

Parameter Sensitivity Analysis

As the hydrophobic excipients or their proportions in an emulsion are varied, API solubility in the dispersed phase may change. The model captures this in the parameter $K_{disp,w}$, the API's dispersed phase — water partition coefficient. Increasing $K_{disp,w}$ (at constant API loading in the formulation) drives more API into the dispersed phase, reducing its fractional saturation in both the continuous and dispersed phases, thereby reducing the driving force for transfer of API to the SC.

The sensitivity of simulated CP dermis concentration-time profiles at mean dOFM probe skin depth (dermis sub-layer 14) on $K_{disp,w}$ is shown in Fig. 3a. The predicted concentrations declined progressively as the value of $K_{disp,w}$ increased from $K_{veg\ oil,w}$ (~ 357) to $K_{o,w}$ (~ 3162). The profiles for different values of $K_{disp,w}$ all have the same shape. When the plotted curves are normalized by their respective values of CP fractional saturation, $F_{sat}(t_0)$ in the formulations (see Equation (10) in the Supplementary Information), the resulting profiles overlap, differing by less than 3% at all simulated times. This result holds, in part, because in each case less than 2% of the CP dose was delivered over 24 hours (CP F_{sat} remained nearly constant), and because changes in the formulation due to evaporative water loss were not simulated (in particular the increase in CP solubility in the continuous phase and reduction in continuous phase volume fraction, j_{cont}).

We also considered the sensitivity of CP concentrations in the dermis to the volume fraction of the dispersed phase,

φ_{disp}. In general, this parameter should be varied only over a range in which an emulsion formulation retains its original phase structure. Variations in φ_{disp} were made by 25% around its model value of 0.244, while assuming that these compositions lie within the O/W emulsion region of the Dermovate cream phase diagram, which has not been reported in the literature. Dose volume was held constant in these simulations, under the assumption that the densities of the continuous and dispersed phases were sufficiently close.

Qualitatively, sensitivity to φ_{disp} was similar to that of $K_{disp,w}$. As shown in Fig. 3b, if φ_{disp} increases, the dispersed phase holds a greater fraction of the CP dose, and fractional saturation in the continuous phase declines, driving lower flux into the SC. For hydrophilic APIs, changing the volume fraction of the dispersed phase in an O/W ME would produce the opposite effect. In the general case, the sensitivity is determined quantitatively by the ratio of API solubilities in the continuous and dispersed phases, which approximates $K_{disp,cont}$.

To illustrate the simulation of a multi-factorial designed experiment, a coupled PSA of $K_{disp,w}$ and φ_{disp} was conducted, in which the $AUC_{0\text{-}24h}$ of the unbound CP concentration-time profile at mean probe depth served as the output. Results of this analysis are summarized in Fig. 3c, which shows the systematic decline in $AUC_{0\text{-}24h}$ as φ_{disp} and $K_{disp,w}$ increased (filled symbols). The simulation results are well described by the response surface (dotted lines) defined in Eq. (1), which provides AUC predictions at interpolated values of (j_{disp}, $K_{disp,w}$). The surface is nonlinear in both parameters, and sensitivity varies with position on the surface.

C_{fmln} is CP concentration in the formulation (held constant across simulations), $C_{int,w}$ is CP intrinsic solubility in water (the reference phase), and $a = AUC_{0\text{-}24h}/F_{sat}(t_0)$ for the simulation using tabulated formulation parameters. The second term on the right-hand side is the initial fractional saturation of CP in the formulation for a given value of $K_{cont,w}$, $K_{disp,w}$, and j_{disp}. The response surface can be used to define regions of ($K_{disp,w}$, j_{disp}) formulation space that produce the same $AUC_{0\text{-}24h}$ within a given tolerance.

$$AUC_{0-24h}\left(K_{disp,w}, \varphi_{\ disp}\right) = a\frac{{}^{C_{fmIn}/C_{int,w}}}{K_{cont,w}(1\ \ \varphi-)\ +\ K_{disp,\ \varphi\ wdisp}} \quad (1)$$

The effective diffusivity of an API in the emulsion continuous phase, D_{eff}, was another parameter for which a plausible range of values was identified. As described above, we derived values that covered more than two orders of magnitude. Moreover, D_{eff} can be affected by formulation attributes such as presence of a gelling polymer, vehicle viscosity, and the dispersed phase volume fraction of emulsions. Hence, we conducted a PSA of D_{eff} covering the range 1e-6 to 1e-11 cm^2/s in order to assess its effect on delivery of CP to the dermis.

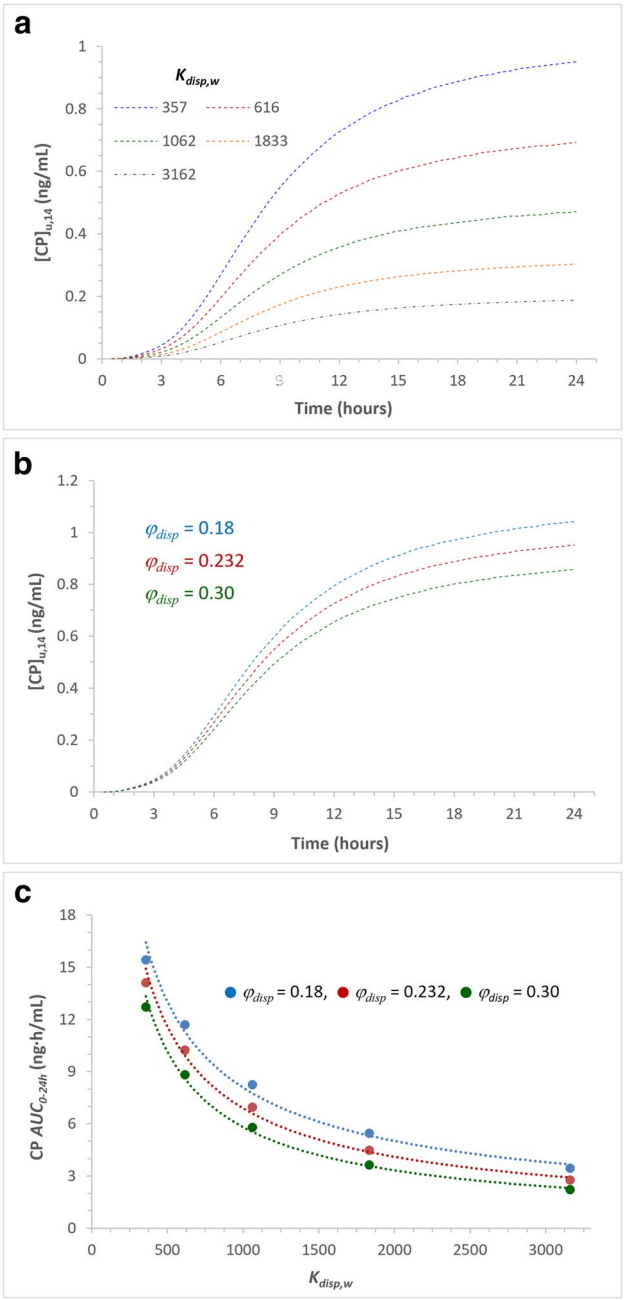

Fig. 3 **a** and **b** Unbound dermis CP concentration-time profiles at mean dOFM probe depth (dermis sub-layer 14) as a function of $K_{disp,w}$ and φ_{disp}, respectively, with model input values unchanged for all other parameters, and **c** Unbound dermis CP $AUC_{0\text{-}24h}$ as a function of CP $K_{disp,w}$ for variations of the φ_{disp} in the formulation. Filled circles represent simulation output; dotted lines represent the surface described in the text

Results of the PSA are shown in Fig. 4. Sensitivity of CP skin permeation was modest. Reducing D_{eff} from 1e-8 to 1e-11 cm^2/s produced only a 40% change in $AUC_{0\text{-}24h}$ at mean probe depth in the dermis. Nonetheless, this is useful information as it suggests a degree of latitude in the

composition of the continuous phase; for example, in the choice of aqueous co-solvent, or use of a gelling polymer, both of which may affect D_{eff} (and reflected on formulation rheology, which can be a drug product critical quality attribute).

The sensitivity of model predictions to D_{eff} can be understood qualitatively by noting that as D_{eff} declines, slow CP transport in the emulsion continuous phase begins to limit the rate of mass transfer into the SC and sebum. This is the hallmark of controlled release formulations. The onset and extension of formulation control occur as the value of $1/P_n^{fmln}$ approaches and then exceeds first the value of $1/P_1^{Sebum}$ in the coefficient K_{mt} in the equation for mass transfer between the formulation and sebum, and then the value of $1/P_1^{SC}$ in K_{mt} for mass transfer between the formulation and SC (see Eq. (9) in the Supplementary Information).

Lastly, the sensitivity of predicted dermis CP concentrations to variation in the radius of spherical droplets of the dispersed phase, r_{disp}, was examined. For the neutral hydrophobic excipients of Dermovate cream, the radius is largely determined by the extent to which those excipients reduce the interfacial free energy per unit area of aggregated excipient molecules and by geometric constraints arising from excipient sizes and shapes [38, 39].

A range of values from 0.1 to 10 mm was explored, the limits being order of magnitude changes from the baseline value. This is much greater, for example, than the 2 to 3-fold difference between d_{10} and d_{90} of the droplet size distribution in metronidazole creams reported by Murthy *et al.* [40]. As r_{disp} varied, we found less than a 1% difference among the unbound CP concentration-time profiles calculated at mean dOFM probe depth. Moreover, regardless of the value of r_{disp}, CP fractional saturation in the continuous and dispersed phases of the formulation also differed by less than 1% at all simulated times. Thus, for each value of r_{disp}, equilibration of CP between the formulation phases was significantly more rapid than CP transport from the formulation into SC and sebum (see Equations (4)–(7) in the Supplementary Information). This is not surprising considering the much faster diffusion of CP in the formulation than through the SC (see Table II).

Publicly available experimental data characterizing rates of water evaporation from Dermovate cream appear to be unavailable. Kasongo measured CP release *in vitro* with and without occlusion [15], with the similarity of the resulting profiles suggesting slow evaporation of water. However, far more cream was applied *in vitro* than clinically; 150 mg/cm^2 *vs* 15 mg/cm^2. Thus, the relevance of Kasongo's measurements for the clinical setting is not clear.

In the absence of measured evaporative water loss data from the clinical setting, one can estimate the effect of such loss on CP skin permeation by simulating the formulations

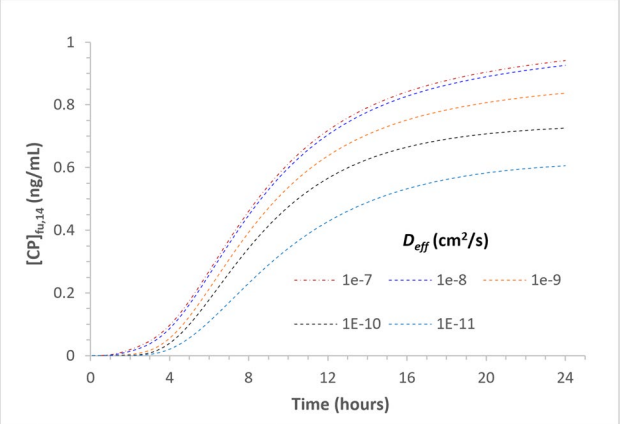

Fig. 4 The dependence of unbound CP concentration-time profiles at mean dOFM probe depth on D_{eff}, the effective diffusivity of CP in the continuous phase of Dermovate cream. The range of estimated values was 4.50e-9–7.56e-7 cm^2/s, with the model input value set to 2.61e-8 cm^2/s. The simulation for D_{eff} = 1e-6 cm^2/s has been omitted for clarity; its predicted dermis CP profile overlaps that for D_{eff} = 1e-7 cm^2/s

that result from fixed reductions in water content relative to Dermovate cream. Model input parameters whose values change under these scenarios include continuous phase volume and j_{cont}, CP solubility in the continuous phase (combining Kasongo's and Fauzee's measurements, ln $C_{sat,cont}$ = 3.93e-3 + 7.69e-2·PG vol%), $K_{cont,w}$, D_{eff}, due to both the increasing viscosity of the binary solvent [19] and the increase in j_{disp} [20]. The values for a series of formulations in which water content was reduced progressively are listed in Table III, and simulated CP concentration-time profiles at mean dOFM probe skin depth are presented in Fig. 5.

Table III indicates that as formulation water content was reduced, CP solubility in the continuous phase, $K_{cont,w}$, and the concentration of CP in the formulation as a whole increased, while formulation volume, D_{eff}, and F_{sat} decreased. Rates of CP skin permeation declined monotonically with reduced formulation water content, suggesting that evaporative water loss from Dermovate cream would reduce the rates of CP skin permeation measured *in vitro* and *in vivo*, although PG skin permeation and potential changes in the phase structure of the formulations at reduced water content were not accounted for in the simulations.

Considering the results in terms of CP concentration in the formulations, $[CP]_{Fmln}$, the model predicted declining rates of CP skin permeation with increasing CP concentration. This result illustrates the point that permeant concentration and fractional saturation in a formulation may diverge in their relationships to thermodynamic activity, the driving force for partitioning into the skin [41, 42]. The model predicts that across this range of formulation changes, fractional saturation is more indicative of this underlying thermodynamic activity. It also illustrates the

Table III Changes in Model Input Parameter Values as the Water Content of Dermovate Cream Declines. %PG is with respect to the continuous phase of the O/W emulsion, not the formulation as a whole. Concentration and solubility, volume, and diffusivity units are mg/mL, mL, and cm^2/s, respectively

% Loss (v/v)	% PG (v/v)	CP Solubility	$K_{cont,w}$	$Volume_{Fmln}$	$[CP]_{Fmln}$	D_{eff}	j_{cont}	j_{disp}	F_{sat}
0	60	0.397	97.7	0.1162	4.97E-01	2.61E-08	0.756	0.244	0.761
10	62.5	0.481	118.4	0.113	5.12E-01	2.37E-08	0.749	0.251	0.708
20	65.2	0.592	145.9	0.109	5.29E-01	2.13E-08	0.741	0.259	0.649
30	68.2	0.744	183.3	0.106	5.46E-01	1.89E-08	0.732	0.268	0.586
40	71.4	0.955	235.3	0.102	5.65E-01	1.66E-08	0.723	0.277	0.518
50	75.0	1.26	309.7	0.099	5.85E-01	1.43E-08	0.713	0.287	0.446
60	78.9	1.70	419.5	0.095	6.07E-01	1.20E-08	0.702	0.298	0.373
70	83.3	2.39	587.8	0.092	6.30E-01	9.87E-09	0.691	0.309	0.300
80	88.2	3.48	856.9	0.0882	6.55E-01	7.79E-09	0.679	0.321	0.232
90	93.8	5.32	1310	0.0847	6.82E-01	5.83E-09	0.665	0.335	0.170
100	100	8.60	2118	0.0812	7.12E-01	4.04E-09	0.651	0.349	0.117

need to think through how changes in the characteristics of complex formulations post application (metamorphosis) are brought about and interrelated.

From the perspective of $K_{cont,w}$, the PSA outcomes reflect how this parameter changes as the formulation as a whole evolves during evaporation. Thus, the similarity of the results shown in Fig. 5 and those of the $K_{disp,w}$ PSA, shown in Fig. 3a, is not surprising, with CP $AUC_{0\text{-}24h}$ showing the same linear relationship to F_{sat} in both cases.

As assessed by skin blanching and other techniques, CP has been shown to be a highly potent vasoconstrictor, with average blanching scores based on a 0–4 categorical scale reaching 50% of their maximal possible value after 6 h of exposure (at which time formulations were removed), and about 80% after 12–14 h, regardless of occlusion status [43–45]. However, the extent of blanching was not related quantitatively to skin blood flow rates. Nonetheless, vasoconstrictive effects can be investigated by assessing the sensitivity of dermis CP concentrations to the changes on local blood flow, Q_{dermis} (mL/min/g skin).

The effects of reductions in Q_{dermis} on dermis CP concentrations were simulated from its baseline value in the human arm, 9.89e-2 to 1e-2 mL/min/g skin. Results of these simulations are plotted in Fig. 6. Reducing Q_{dermis} raised dermis CP concentrations progressively over simulated time, an effect that presumably saturates *in vivo* as blanching does with increasing corticosteroid dose [46]. Thus, within the scope of the current assumptions, vasoconstriction and evaporative water loss have opposing effects of CP skin permeation and may also act over differing timescales. How these affect CP skin permeation in clinical settings remains to be elucidated.

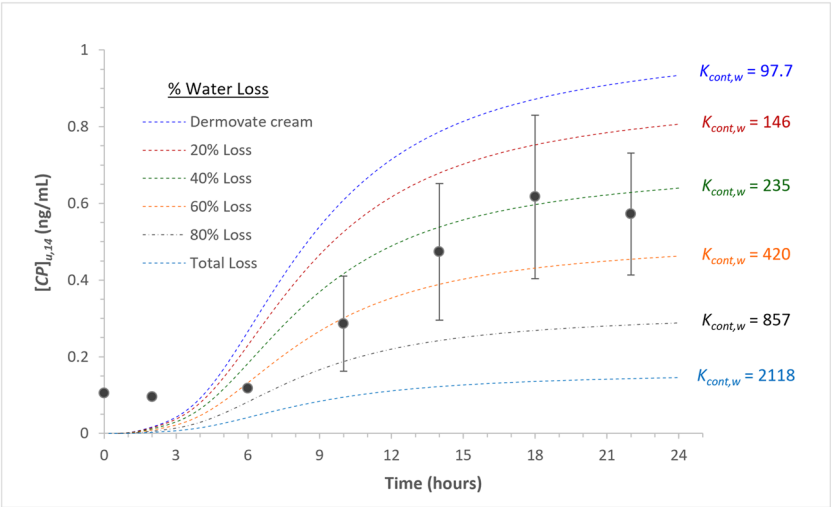

Fig. 5 The effect of stepwise reductions in the water content of Dermovate cream on the unbound concentration of CP in dermis sub-layer 14 from 0 to 24 h. The clinical data are included for reference. Values of the CP continuous phase–water partition coefficient, $K_{cont,w}$, for the sequence of formulation states are listed to the right of each curve

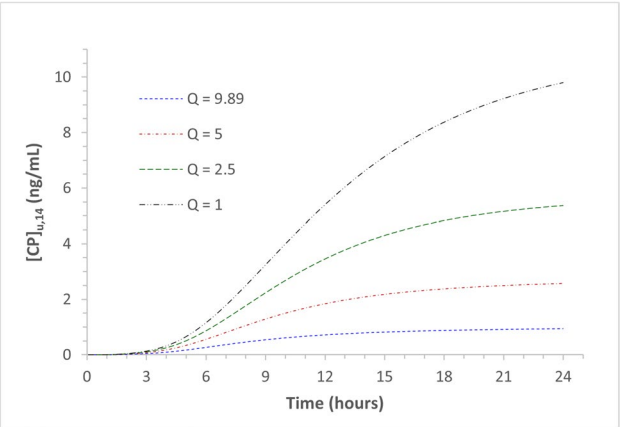

Fig. 6 The effect of dermis blood flow rate, Q_{dermis} on unbound CP concentrations-time profiles at mean probe depth (dermis sub-layer 14) as the rate was reduced from the model arm skin physiology value of 9.89e-2 mL/min/g of skin

Discussion

In this work, a dermal PBPK model was developed to describe the permeation through the skin of CP following the application of Dermovate cream in virtual healthy subjects. Sufficient experimental characterization of Dermovate cream, an emulsion-based formulation of CP, was available to support model development for topical delivery of this steroid. For some model inputs, a range of plausible values were derived from the available data. In such cases, we selected specific values in these ranges to develop a skin absorption model and generate reasonable predictions of CP dermis concentration-time profiles. The sensitivity of model predictions to these parameters and drug product quality attributes was then investigated.

Within the scope of model validation, the "bottom-up" model predictions were compared against CP dermis concentration–time profiles measured on Day 1 of a 14-day clinical study conducted by Bodenlenz *et al.* [11]. Model predictions of unbound dermis CP concentrations and $AUC_{u,24h}$ measured by dOFM were reasonably accurate with respect to time and probe skin depth which was provided by the authors. The model was able to capture the inverted relationship between CP dermis exposure and probe skin depth that was also reported by Bodenlenz *et al.* which enforces the credibility of the developed model. The model predicted less than 2% of the dose is delivered over 24 h, hence it also predicted a long quasi-steady state extending from 7 to 10 days. By leveraging the versatile capabilities of the GastroPlus population simulator, the developed and validated model can be used to inform study design decisions related to application duration, dose application and required number of study participants for prospective dOFM studies with the Dermovate cream in a population of healthy volunteers.

Additionally, the acceptable performance of the model against observed dOFM data collected in non-lesional skin of psoriatic patients is a promising finding. The validated model described the interaction between a topical drug product (topical cream) and the non-lesional skin well. As such, this model may be considered as the first step towards the development and validation of a disease skin model for psoriatic patients that may be used to support drug product development by guiding *in vivo* testing for the Dermovate cream or other therapeutic options for the psoriatic patient population. Obviously, the pathophysiology of psoriatic skin will need to be informed in the model and any potential diseased skin to drug product interaction will need to be assessed anew.

Using the validated model, PSA revealed considerable dependence of dermis concentration profiles on P_{sebum}, dermis blood flow (Q_{dermis}), and dispersed phase-water partition coefficient ($K_{disp,w}$), but modest dependence on dispersed phase volume fraction, j_{disp}, CP effective diffusivity in the continuous phase of the formulation (D_{eff}), and negligible dependence on the mean radius of dispersed phase droplets (r_{disp}). Thus, given the default physiology of human arm skin in the model, the simulated performance of the formulation was more sensitive to its thermodynamic properties than its transport properties. This may not always be the case. The transport properties of a formulation might limit the transdermal flux of a compound having high SC permeability. The determining factor will often, but not inevitably, be the balance between formulation and SC permeabilities.

PSA can be thought of as a kind of computational QbD tool that allows for conducting factorial experiments *in silico* to elucidate the contributions of formulation attributes to the delivery of an API when an appropriately validated model is available. Parameter sensitivity can be evaluated in some cases quantitatively ($K_{disp,w}$ and j_{disp}), in other cases qualitatively (D_{eff}), via the equations for mass exchange between formulation and skin towards decision making pertaining to formulation development and selection.

It is important to note several assumptions that were made during model development and other relevant limitations of the model. Firstly, although the dOFM data that were used for model validation were collected following drug product application on the non-lesional skin of psoriatic patients, model predictions were generated in skin of healthy virtual subjects with no skin disease present. This choice was made due to an absence of consensus in the literature; there are conflicting data on whether properties of non-lesional psoriatic skin physiology such as trans-epidermal water loss, SC hydration, and erythema index are significantly different than healthy skin [47–49]. As the physiological properties of psoriatic lesions become better understood and incorporated into the computational model, the model may be extendable to simulation of permeation through lesional psoriatic skin.

CP may provide a valuable case study to assess the critical properties of lesional psoriatic skin leading to changes in skin permeation.

Secondly, in the developed model dynamic drug product evaporation was not simulated, due to limitations in the current implementation of the model, and CP solubility remained unchanged post application. To investigate the effects of evaporative water loss, a set of simulations was conducted at sequentially reduced formulation water content, with API solubility and diffusivity in the continuous phase updated accordingly. From these calculations, we conclude that the dynamic treatment of formulation evolution requires an expanded computational model to include updating API solubility and diffusivity in the phases of a formulation as (i) water and perhaps other solvents (e.g., ethanol, PG) evaporate or permeate the skin; (ii) concentrations of polymers, if present, rise; and in emulsion-based formulations (iii), dispersed phase volume fraction rises or (iv) phase structure changes. In the absence of experimentally measured API solubility as a function of solvent composition, predictive thermodynamics methods are available [50–52]. Concomitantly, the model can be extended to track the skin permeation of additional molecular species (e.g., surfactants, co-surfactants) to encompass the possibility of API enhancement permeation.

Conclusions

In summary, the present work involves a skin absorption model validated against dOFM data. The dermal PBPK model described well CP permeation through non-lesional skin of psoriatic patients. This PBPK modeling approach appears to be a promising approach in studying the sensitivity of drug absorption and disposition in the skin to changes in the thermodynamic and transport properties of topical formulations, particularly in relation to rate-limiting steps in API skin permeation. The sensitivity of API skin permeation to formulation attributes can be assessed for single parameters, and the combined effects of multiple parameters can be quantified through coupled PSA, while bearing in mind the physical co-dependencies among parameters. This approach may inform the design of both new and generic formulations applied on the skin.

Supplementary Information The online version contains supplementary material available at https://doi.org/10.1208/s12249-024-02740-x.

Author Contribution WvO and JN built the clobetasol model and conducted the simulations. WvO, JN, MLM, JS, and ET drafted the manuscript. All authors provided manuscript review and revisions.

Funding This publication has been supported by the Food and Drug Administration (FDA) of the U.S. Department of Health and Human Services (HHS) as part of financial assistance awards 1 U01 FD006526-01 and 1 U01 FD007320-01 totaling $1M with 100 percent funded by FDA/HHS.

Declarations

Conflict of Interest WvO, JN, MLM, JS, and VL are current employees of Simulations Plus, Inc. and may be shareholders. The contents are those of the author(s) and do not necessarily represent the official views of, nor an endorsement, by FDA/HHS, or the U.S. Government.

References

1. Mian M, Silfvast-Kaiser A, Paek S, Kivelevitch D, Menter A. A review of the most common dermatologic conditions and their debilitating psychosocial impacts. Int Arch Intern Med. 2019;22:3.
2. Tsakalozou E, Babiskin A, Zhao L. Physiologically-based pharmacokinetic modeling to support bioequivalence and approval of generic products: a case for diclofenac sodium topical gel,1%. CPT: Pharmacometrics & Systems Pharmacology [Internet]. [cited 2021 Feb 8];n/a(n/a). Available from: https://ascpt.onlinelibrary.wiley.com/doi/abs/10.1002/psp4.12600.
3. FDA. Draft guidance on diclofenac sodium [Internet]. 2011. Available from: https://www.accessdata.fda.gov/drugsatfda_docs/psg/Diclofenac%20Sodium_draft_Topical%20gel_RLD%2022122_RC07-18.pdf.
4. FDA. Draft guidance on clobetasol propionate [Internet]. 2011. Available from: https://www.accessdata.fda.gov/drugsatfda_docs/psg/Clobetasol_Propionate_fmaerosol_21142_RC2-11.pdf.
5. Ghosh P, Raney SG, Luke MC. How does the Food and Drug Administration approve topical generic drugs applied to the skin? Dermatol Clin. 2022;40(3):279–87.
6. Raney SG, Franz TJ, Lehman PA, Lionberger R, Chen ML. Pharmacokinetics-based approaches for bioequivalence evaluation of topical dermatological drug products. Clin Pharmacokinet. 2015;54(11):1095–106.
7. FDA. FY 2022 GDUFA science and research report [Internet]. FDA; 2023 Feb. (GDUFA Science and Research Reports). Available from: https://www.fda.gov/drugs/generic-drugs/fy-2022-gdufa-science-and-research-report.
8. Yuvaneshwari K, Sivacharan K, Tausif A, Siddharth C. Applications of PBPK/PBBM modeling in generic product

development: an industry perspective. Journal of Drug Delivery Science and Technology. 2022 Mar;69.
9. Tsakalozou E, Alam K, Babiskin A, Zhao L. Physiologically-based pharmacokinetic modeling to support determination of bioequivalence for dermatological drug products: scientific and regulatory considerations. Clinical Pharmacology & Therapeutics [Internet]. Available from: https://onlinelibrary.wiley.com/doi/abs/10.1002/cpt.2356.
10. CDER FY 2022 GDUFA science and research report. Available from: https://www.fda.gov/media/164843/download.
11. Bodenlenz M, Dragatin C, Liebenberger L, Tschapeller B, Boulgaropoulos B, Augustin T, et al. Kinetics of clobetasol-17-propionate in psoriatic lesional and non-lesional skin assessed by dermal open flow microperfusion with time and space resolution. Pharm Res. 2016;33(9):2229–38.
12. Dermovate_Cream_and_Ointment_GDS12-IPI_05_1_03_2019.pdf [Internet]. [Available from: https://gskpro.com/content/dam/global/hcpportal/en_BD/PI/Dermovate_Cream_and_Ointment_GDS12-IPI_05_1_03_2019.pdf.
13. 019322Orig1s000rev.pdf [Internet]. [cited 2022 Jul 5]. Available from: https://www.accessdata.fda.gov/drugsatfda_docs/nda/pre96/019322Orig1s000rev.pdf.
14. Sangster JM. Octanol-water partition coefficients: fundamentals and physical chemistry. John Wiley & Sons, Inc; 1997.
15. Kasongo KW. Development and in vitro evaluation of a clobetasol 17-propionate topical cream formulation [Master of Science (Pharmacy)]. [Grahamstown, South Africa]: Rhodes University; 2007.
16. Fauzee AFB. Development, manufacture and assessment of clobetasol 17-propionate cream formulations [Master of Science (Pharmacy)]. [Grahamstown, South Africa]: Rhodes University; 2011.
17. Otto A, Wiechers JW, Kelly CL, Dederen JC, Hadgraft J, du Plessis J. Effect of emulsifiers and their liquid crystalline structures in emulsions on dermal and transdermal delivery of hydroquinone, salicylic acid and octadecenedioic acid. Skin Pharmacol Physiol. 2010;23(5):273–82.
18. Siepmann J, Peppas NA. Higuchi equation: derivation, applications, use and misuse. Int J Pharm. 2011;418(1):6–12.
19. Khattab IS, Bandarkar F, Khoubnasabjafari M, Jouyban A. Density, viscosity, surface tension, and molar volume of propylene glycol+water mixtures from 293 to 323K and correlations by the Jouyban-Acree model. Arab J Chem. 2017;1(10):S71-5.
20. Cheng SC, Vachon RI. The prediction of the thermal conductivity of two and three phase solid heterogeneous mixtures. Int J Heat Mass Transfer. 1969;12(3):249–64.
21. Crank J. The mathematics of diffusion. 2d ed. Oxford, [Eng]: Clarendon Press; 1975. Chapter 12.
22. Zhang J, Michniak-Kohn B. Investigation of microemulsion microstructures and their relationship to transdermal permeation of model drugs: ketoprofen, lidocaine, and caffeine. Int J Pharm. 2011;421(1):34–44.
23. Ahmedi R, Lanez T. Experimental partition determination of octanol-water coefficients of ferrocene derivatives using square wave voltammetry techniques. J Fundam Appl Sci. 2018;10(1):308–27.
24. Wilschut A, ten Berge WF, Robinson PJ, McKone TE. Estimating skin permeation. The validation of five mathematical skin permeation models. Chemosphere. 1995;30(7):1275–96.
25. Kretsos K, Miller MA, Zamora-Estrada G, Kasting GB. Partitioning, diffusivity and clearance of skin permeants in mammalian dermis. Int J Pharm. 2008;346(1–2):64–79.
26. Siddiqui O, Roberts MS, Polack AE. Percutaneous absorption of steroids: relative contributions of epidermal penetration and dermal clearance. J Pharmacokinet Biopharm. 1989;17(4):405–24.
27. Hansch C, Leo A, Hoekman D. Exploring QSAR: Volume 2: hydrophobic, electronic, and steric constants. 1st edition. Washington, DC: American Chemical Society; 1995.
28. Yang S, Li L, Lu M, Chen T, Han L, Lian G. Determination of solute diffusion properties in artificial sebum. J Pharm Sci. 2019;108(9):3003–10.
29. Yang S, Li L, Chen T, Han L, Lian G. Determining the effect of pH on the partitioning of neutral, cationic and anionic chemicals to artificial sebum: new physicochemical insight and QSPR model. Pharm Res. 2018;35(7):141.
30. Hehir M, Du Vivier A, Eilon L, Danie MJ, Shenoy EV. Investigation of the pharmacokinetics of clobetasol propionate and clobetasone butyrate after a single application of ointment. Clin Exp Dermatol. 1983;8(2):143–51.
31. van Velsen SGA, De Roos MP, Haeck IM, Sparidans RW, Bruijnzeel-Koomen CAFM. The potency of clobetasol propionate: serum levels of clobetasol propionate and adrenal function during therapy with 0.05% clobetasol propionate in patients with severe atopic dermatitis. J Dermatolog Treat. 2012;23(1):16–20.
32. Bodenlenz M, Aigner B, Dragatin C, Liebenberger L, Zahiragic S, Höfferer C, et al. Clinical applicability of dOFM devices for dermal sampling. Skin Res Technol. 2013;19(4):474–83.
33. Gaigalas AK, Hubbard JB, McCurley M, Woo S. Diffusion of bovine serum albumin in aqueous solutions. J Phys Chem. 1992;96(5):2355–9.
34. Ramanujan S, Pluen A, McKee TD, Brown EB, Boucher Y, Jain RK. Diffusion and convection in collagen gels: implications for transport in the tumor interstitium. Biophys J. 2002;83(3):1650–60.
35. Kretsos K, Kasting GB. Dermal capillary clearance: physiology and modeling. Skin Pharmacol Physiol. 2005;18(2):55–74.
36. Cevc G, Vierl U. Spatial distribution of cutaneous microvasculature and local drug clearance after drug application on the skin. J Control Release. 2007;118(1):18–26.
37. Calcutt JJ, Roberts MS, Anissimov YG. Predicting viable skin concentration: modelling the subpapillary plexus. Pharm Res. 2022;39(4):783–93.
38. Israelachvili JN, Mitchell DJ, Ninham BW. Theory of self-assembly of hydrocarbon amphiphiles into micelles and bilayers. J Chem Soc, Faraday Trans 2. 1976;72(0):1525–68.
39. Tartaro G, Mateos H, Schirone D, Angelico R, Palazzo G. Microemulsion microstructure(s): a tutorial review. Nanomaterials (Basel). 2020;10(9):E1657.
40. Murthy SN. Characterizing the critical quality attributes and in vitro bioavailability of acyclovir and metronidazole topical products [Internet]. Available from: https://www.fda.gov/media/110262/download.
41. Bunge AL, Persichetti JM, Payan JP. Explaining skin permeation of 2-butoxyethanol from neat and aqueous solutions. Int J Pharm. 2012;435(1):50–62.
42. Frasch HF, Barbero AM, Dotson GS, Bunge AL. Dermal permeation of 2-hydroxypropyl acrylate, a model water-miscible compound: effects of concentration, thermodynamic activity and skin hydration. Int J Pharm. 2014;460(1–2):240–7.
43. Meyer E, Magnus AD, Haigh JM, Kanfer I. Comparison of the blanching activities of Dermovate, Betnovate and Eumovate creams and ointments. International Journal of Pharmaceutics. 1988;41(1):63–6.

44. Emtestam L, Kuzmina N, Talme T. Evaluation of the effects of topical clobetasol propionate by visual score, electrical impedance and laser Doppler flowmetry. Skin Res Technol. 2007;13(1):73–8.
45. Queille-Roussel C, Bang B, Clonier F, Lacour JP. Enhanced vasoconstrictor potency of the fixed combination calcipotriol plus betamethasone dipropionate in an innovative aerosol foam formulation vs. other corticosteroid psoriasis treatments. J Eur Acad Dermatol Venereol. 2016;30(11):1951–6.
46. Topical Dermatologic Corticosteroids: In Vivo Bioequivalence [Internet]. 2022. Available from: https://www.fda.gov/regulatory-information/search-fda-guidance-documents/topical-dermatologic-corticosteroids-in-vivo-bioequivalence-0.
47. Takahashi H, Tsuji H, Minami-Hori M, Miyauchi Y, Iizuka H. Defective barrier function accompanied by structural changes of psoriatic stratum corneum. J Dermatol. 2014;41(2):144–8.
48. Maroto-Morales D, Montero-Vilchez T, Arias-Santiago S. Study of skin barrier function in psoriasis: the impact of emollients. Life. 2021;11(7):651.
49. Montero-Vilchez T, Segura-Fernández-Nogueras MV, Pérez-Rodríguez I, Soler-Gongora M, Martinez-Lopez A, Fernández-González A, et al. Skin barrier function in psoriasis and atopic dermatitis: transepidermal water loss and temperature as useful tools to assess disease severity. J Clin Med. 2021;10(2):359.
50. Miller MA, Kasting GB. A spreadsheet-based method for simultaneously estimating the disposition of multiple ingredients applied to skin. J Pharm Sci. 2015;104(6):2047–55.
51. Gmehling J, Constantinescu D, Schmid B. Group contribution methods for phase equilibrium calculations. Annu Rev Chem Biomol Eng. 2015;6:267–92.
52. Klamt A, Eckert F, Arlt W. COSMO-RS: an alternative to simulation for calculating thermodynamic properties of liquid mixtures. Annu Rev Chem Biomol Eng. 2010;1:101–22.